

Example of a first-order Néel to valence-bond-solid transition in two dimensions

Arnab Sen and Anders W. Sandvik

Department of Physics, Boston University, 590 Commonwealth Avenue, Boston, Massachusetts 02215, USA

(Received 8 September 2010; published 22 November 2010)

We consider the $S=1/2$ Heisenberg model with nearest-neighbor interaction J and an additional multispin interaction Q_3 on the square lattice. The Q_3 term consists of three bond-singlet projectors and is chosen to favor the formation of a valence-bond solid (VBS) where the valence bonds (singlet pairs) form a staggered pattern. The model exhibits a quantum phase transition from the Néel state to the VBS as a function of Q_3/J . We study the model using quantum Monte Carlo (stochastic series expansion) simulations. The Néel-VBS transition in this case is strongly first order in nature, in contrast to similar previously studied models with continuous transitions into columnar VBS states. The qualitatively different transitions illustrate the important role of an emerging $U(1)$ symmetry in the latter case, which is not possible in the present model due to the staggered VBS pattern (which does not allow local fluctuations necessary to rotate the local VBS order parameter).

DOI: [10.1103/PhysRevB.82.174428](https://doi.org/10.1103/PhysRevB.82.174428)

PACS number(s): 75.10.Jm, 75.10.Nr, 75.40.Mg, 75.40.Cx

I. INTRODUCTION

Even though quantum phase transitions (QPTs) occur strictly at zero temperature (T), they can strongly influence the behavior of a system at $T>0$ in their vicinity.¹ Exotic QPTs that do not have any analogs in classical critical phenomena may thus leave widely observable signatures. A very interesting example of such a QPT was proposed by Senthil *et al.*,² who reconsidered the transition between Néel and valence-bond-solid (VBS) phases in two-dimensional (2D) square lattice $S=1/2$ antiferromagnetic spin systems.^{3,4} They argued that subtle Berry phase effects can lead to an unconventional “deconfined” quantum-critical (DQC) transition that is generically continuous while a standard Landau-Ginzburg-Wilson analysis would instead predict a first-order transition (except at fine-tuned multicritical points) since the two phases break unrelated symmetries. At the DQC point, new fractionalized degrees of freedom (DOFs), $S=1/2$ spinons, become liberated² while they are confined in the conventional phases on either side of the transition.

An important question raised by the field-theoretical work on DQC points² is whether there are microscopic models (Hamiltonians) where the existence of this unconventional quantum criticality can be explicitly demonstrated. Such models, apart from allowing unbiased tests of the validity of the concept, can lead to further theoretical developments. This is also important in view of the work reported by Kuklov *et al.* in Refs. 5 and 6, where an action claimed to realize the low-energy physics of the noncompact (NC) CP^1 field theory, argued by Senthil *et al.*² to describe the DQC point, was studied using Monte Carlo simulations of three-dimensional classical current models with easy-plane and $SU(2)$ symmetries. The transitions in both cases were argued to be generically weakly first order, in contradiction with the proposal of Ref. 2. Other, similar studies have given different results, however.^{7,8} A full understanding of the NCCP¹ theory and its ability to capture the physics of the Néel-VBS transition in 2D antiferromagnets is still lacking.

One approach to the DQC problem is to identify and study microscopic quantum spin Hamiltonians exhibiting the Néel-VBS transition. In a recently proposed class of $S=1/2$

“ J - Q ” models,^{9,10} a geometrically unfrustrated multispin interaction of strength Q (consisting of two or more bond-singlet projectors) was introduced which competes with the Heisenberg interaction J . Quantum Monte Carlo (QMC) calculations in this case are free from the sign problems¹¹ hampering studies of frustrated systems (which also exhibit Néel-VBS transitions¹²). Calculations in the ground state^{9,10} and at finite temperature¹³ have demonstrated behaviors consistent with a continuous Néel-VBS transition of the DQC type. In particular, the dynamic exponent $z=1$ and the anomalous dimension associated with the spin correlations is relatively large; $\eta \approx 0.35$.

It has been claimed^{6,14} that scaling corrections in the J - Q model indicate phase coexistence and, thus, an eventual first-order transition. Indeed, a very weak first-order transition can be hard to distinguish from a continuous one on finite lattices. However, using much larger lattices than in Ref. 14, the scaling corrections were later shown¹⁵ to be too weak to be generated by phase coexistence. The behavior instead suggests logarithmic corrections to scaling. Such corrections, which have also been observed by studying the response of the critical spin texture to impurities,¹⁶ raise interesting questions on the presence of marginally irrelevant operators (or, possibly, conventional irrelevant operators with scaling dimension very close to 0) in corresponding field theories. While one still cannot, strictly speaking, rule out an extremely weak first-order transition, there are no concrete indications based on current observations. It can be noted that logarithmic corrections have been found in related gauge theories with fermions.¹⁷

In light of the controversy regarding the nature of the Néel-VBS transition, and in order to gain further insights into the unusual physics of DQC points, it is useful to also study similar transitions that are definitely of first order. This is the topic of the present paper. Ideally, one would like to have a model in which the transition could be tuned from strongly to weakly first order, through a tricritical point into a continuous transition. No such tunable model is known so far, however. In this work, we provide an example of a Néel-VBS transition on the 2D square lattice that is strongly first order. We introduce a J - Q_3 model in which the Q_3 interaction consists of three singlet projectors arranged in a staggered

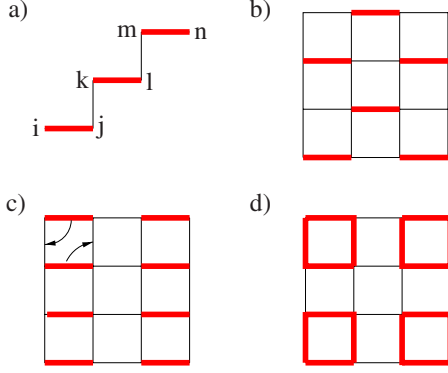


FIG. 1. (Color online) (a) The interaction term Q_3 involving three bond-singlet projection operators (shown with thicker lines) on the square lattice. All terms related by lattice translations and rotations of the shown instance of a product of singlet projectors are included in the Hamiltonian. Examples of VBS patterns: (b) staggered, (c) columnar, and (d) plaquette. The singlets preferentially form on the thicker (red) bonds. The arrows in (c) indicate how a local resonance of a pair of bonds between horizontal and vertical orientations corresponds to a plaquette in (d). Such resonances correspond to fluctuations of the VBS angle, which is $\phi = n\pi/2$ ($n=0,1,2,3$) for the columnar state and $\phi = n\pi/2 + \pi/4$ for the plaquette state. In the DQC scenario (Ref. 2) they lead to an emergent $U(1)$ symmetry, i.e., a continuous circular-symmetric ϕ as the transition into the Néel state is approached. The Q_3 term favors the staggered-type VBS (b), where such angular fluctuations should always be small.

fashion on the square lattice, as illustrated in Fig. 1(a). This interaction induces a staggered VBS pattern in which resonating valence bonds leading locally to a different (degenerate) VBS pattern are not favored. If such fluctuations are present they can effectively rotate the coarse-grained angle of the VBS order parameter (as explained further in the caption of Fig. 1), which has been explicitly observed in the J - Q models studied previously.^{9,10,14} In the DQC scenario, they are directly responsible for the emergent $U(1)$ symmetry of the VBS order parameter in the neighborhood of the transition.² The absence of this feature in the model studied here brings it clearly outside the framework of DQC points, and a numerical confirmation of a different type of transition is then, indirectly, an additional piece of evidence in favor of a consistent DQC scenario in which emergent $U(1)$ symmetry and spinon deconfinement should go hand-in-hand with a continuous transition.

We here use the stochastic series expansion (SSE) QMC method with operator-loop updates¹⁸ to study the nature of the Néel-VBS transition in the staggered J - Q_3 model. We perform simulations at a fixed aspect ratio of inverse temperature $\beta J = L$, as done previously for the standard J - Q_2 model in Refs. 13–15. We study the finite-size scaling properties of various physical quantities and contrast them with what is observed at the previously studied putative continuous DQCs.

The rest of the paper is organized in the following way: in Sec II, we define the model more precisely and present the results for the staggered magnetization, the corresponding Binder cumulant, the spin stiffness, and the VBS order pa-

rameter. We also consider the probability distribution of the VBS order parameter and use it to explicitly demonstrate phase coexistence. In Sec III, we determine the location of the critical point by using the crossing of the energies of the Néel and the VBS phases in the metastable region near the transition. We state our conclusions and discuss future prospects in Sec IV.

II. MODEL AND ORDER PARAMETERS

We consider the following Hamiltonian:

$$H = J \sum_{\langle ij \rangle} \mathbf{S}_i \cdot \mathbf{S}_j - Q_3 \sum_{\langle ijklmn \rangle} C_{ij} C_{kl} C_{mn}, \quad (1)$$

where \mathbf{S}_i refers to a $S=1/2$ spin at site i on the 2D square lattice and C_{ij} denotes the singlet pair projection operator,

$$C_{ij} = \frac{1}{4} - \mathbf{S}_i \cdot \mathbf{S}_j, \quad (2)$$

between two nearest neighbors i and j . The Q_3 term (where, in the notation of Ref. 10, the subscript on Q refers to the number of singlet projectors in the product) is chosen in the particular manner illustrated in Fig. 1(a), to favor the formation of the kind of staggered VBS illustrated in Fig. 1(b). Like the columnar and plaquette VBS, the broken symmetry of the staggered VBS is Z_4 . However, this type of VBS is very different from its columnar or plaquette counterparts since no local ring exchange of singlets on closed loops [e.g., as illustrated in Fig. 1(c) for a simple two-bond resonance] is possible in the *ideal* staggered VBS. This makes it highly unlikely for the existing fluctuations of this kind of VBS to be associated with an emergent $U(1)$ symmetry, which is a key characteristic of the DQC transition.² We will confirm this with simulation results below.

We have also studied an interaction similar to the six-spin Q_3 term but with only two singlet projectors, on two pairs of sites separated by one lattice spacing and shifted one step with respect to each other as in Fig. 1(a). This interaction is not sufficient for destroying the Néel order, however, unlike the original J - Q model with the two singlet projectors inside 2×2 plaquettes. In the latter case the resulting VBS in the extreme case of $J=0$ is also quite weak⁹ while adding one more singlet projector (with the sets of three projectors arranged in columns) gives a much more robust VBS order.¹⁰

To study the Néel-VBS phase transition in the staggered J - Q_3 model, Eq. (1), we measure quantities that are sensitive to the Néel order and the VBS order, respectively. At a continuous quantum phase transition, these quantities should scale with the system size L according to nontrivial critical exponents while at a first-order transition one would expect very different exponents related to the dimensionality of the system as well as particular signatures of coexisting phases at the transition point. These signatures should apply when the linear dimension of the system $L \gtrsim \xi$, where ξ is the finite correlation length at the transition.

A. Néel order

The magnetically ordered Néel phase breaks the $SU(2)$ rotational symmetry of the interaction Hamiltonian H and

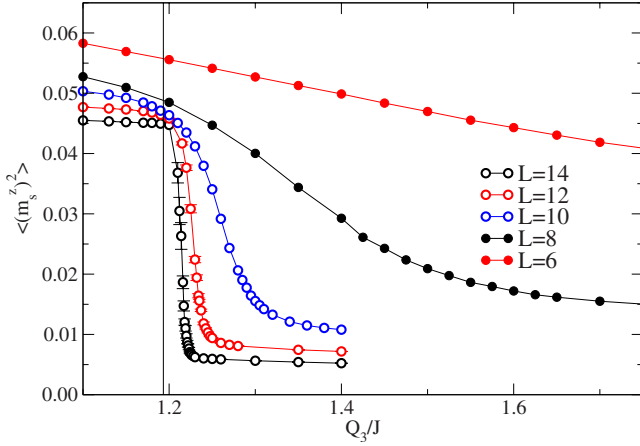


FIG. 2. (Color online) The squared staggered magnetization $\langle (m_s^z)^2 \rangle$ shown for different system sizes at inverse temperature $\beta J = L$. The vertical line at $(Q_3/J)_c = 1.1933$ is the estimated $L \rightarrow \infty$ transition point from crossings of metastable energy branches (Fig. 7).

can be characterized by measuring $\langle (m_s^z)^2 \rangle$, where m_s^z denotes the z component of staggered magnetization of the system,

$$m_s^z = \frac{1}{N} \sum_{\mathbf{r}} S^z(\mathbf{r}) \cos(\mathbf{Q} \cdot \mathbf{r}) \quad (3)$$

with $\mathbf{Q} = (\pi, \pi)$ the wave vector corresponding to the Néel phase and $N = L^2$. This quantity is diagonal in the S^z basis used and can be easily measured in the SSE simulations. We measure the squared quantity $\langle (m_s^z)^2 \rangle$, which, due to the spin-rotational symmetry of the Hamiltonian, is 1/3 of the full squared staggered magnetization $\langle m_s^2 \rangle$. We show the data for different system sizes at $\beta J = L$ near the phase transition in Fig. 2. As the system size is increased, we observe a jump developing in $\langle (m_s^z)^2 \rangle$ that becomes more abrupt and rapidly approaches the infinite-volume estimate of the critical point $(Q_3/J)_c = 1.1933(1)$ for this model (indicated by the vertical line in Fig. 2 and other figures). The value of $(Q_3/J)_c$ was obtained from the crossing of metastable energies of the Néel and VBS phases of larger systems; see Fig. 7 and later discussion in Sec. III. This kind of behavior of the Néel order parameter is already very suggestive of a first-order transition. Data for systems larger than $L = 14$ are not shown here because of the extremely long tunneling times between the coexisting (as we will show below in Sec. II B) Néel and VBS phases for such sizes in our simulations close to the phase transition, which makes it very difficult to obtain reliable expectation values.

A quantity that is very useful for distinguishing between first-order and continuous phase transitions is the Binder cumulant U_2 , defined for an $O(3)$ order parameter as¹⁹

$$U_2 = \frac{5}{2} \left(1 - \frac{\langle (m_s^z)^4 \rangle}{3 \langle (m_s^z)^2 \rangle^2} \right). \quad (4)$$

With the factors used here, $U_2 \rightarrow 1$ in the Néel phase and $U_2 \rightarrow 0$ in the magnetically disordered phase (VBS in this case) when $L \rightarrow \infty$. For a continuous phase transition, the U_2

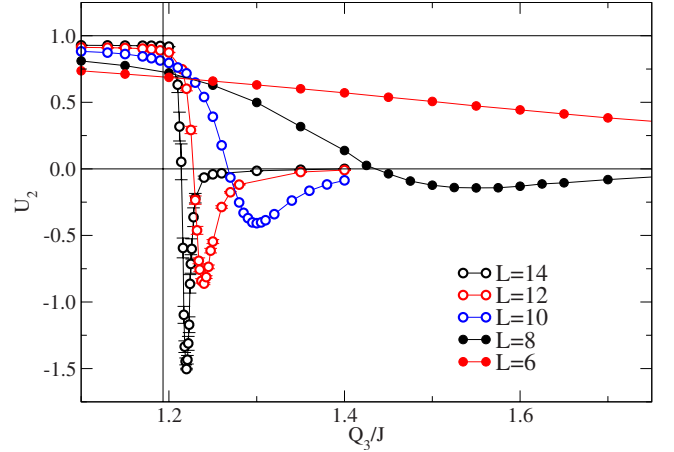


FIG. 3. (Color online) The Binder cumulant of the staggered magnetization shown for different system sizes at inverse temperature $\beta J = L$. Note that the minimum of the Binder cumulant is negative for $L \geq 8$ and diverges to $-\infty$ as $L \rightarrow \infty$ based on these sizes.

curves for different system sizes intersect at the critical point (for sufficiently large L) and the value of U_2 at the intercept normally lies in the interval $(0, 1)$.¹⁹ This property of the Binder cumulant is often used to accurately determine the location of the critical point for continuous phase transitions. However, for a first-order transition, the Binder cumulant behaves in a completely different manner that was explained phenomenologically for classical transitions by Vollmayr *et al.*²⁰ For systems exceeding a certain length $L_{\min} \sim \xi$, the curves show a minimum which becomes more pronounced as the system size increases. The minimum value of $U_2 \rightarrow -\infty$ as $L \rightarrow \infty$ because of phase coexistence, and the position of the minimum approaches the transition point in the thermodynamic limit. This behavior has been observed in previous studies of classical first-order phase transitions [for example, see Refs. 20 and 21]. Indeed, the Binder cumulant for the J - Q_3 model, graphed in Fig. 3, behaves in a similar manner and strongly points to a first-order phase transition. The negative minimum is present in the U_2 curves for $L = 6$ and above and becomes deeper and sharper as L increases. Its location approaches the estimated $(Q_3/J)_c$. The fact that a minimum in U_2 is not at all present for $L = 4$ and is barely negative for $L = 6$ allows us to estimate that the typical length scale (the spin-correlation length) at the first-order transition is approximately in the range $\xi = 4 - 6$. We also measure the second moment spin-correlation length ξ_a defined as

$$\xi_a = \frac{L}{2\pi} \sqrt{\frac{S(\pi, \pi)}{S\left(\pi + \frac{2\pi}{L}, \pi\right)} - 1}, \quad (5)$$

where $S(\mathbf{q})$ refers to the spin structure factor at the corresponding wave vector \mathbf{q} . We obtain $\xi_a \sim 2$ close to the critical point in the magnetically disordered VBS phase. However, when the spin-correlation length is small, ξ_a can differ from the *true* correlation length ξ based on the asymptotic decay of the spin correlations in real space (which is difficult to extract reliably).

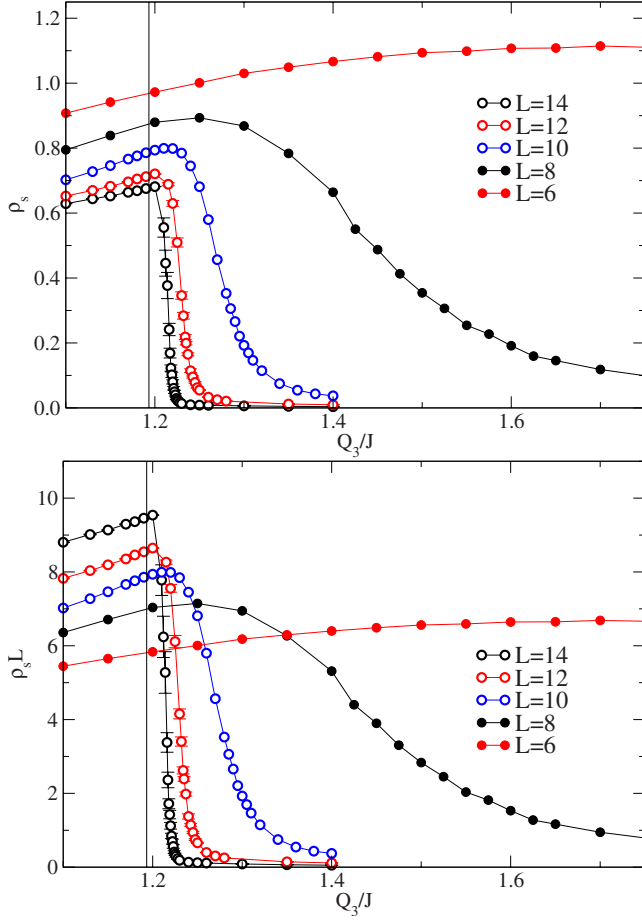


FIG. 4. (Color online) The spin stiffness ρ_s (top panel) and $\rho_s L$ (bottom panel) for different system sizes.

An important quantity characterizing the Néel phase is the spin stiffness ρ_s ; the second derivative of the ground-state energy $E(\phi)$ (per spin) in the presence of a twisted boundary condition (with rotation of a boundary row or column by an angle ϕ),

$$\rho_s = \frac{\partial^2 E(\phi)}{\partial \phi^2}. \quad (6)$$

This quantity is obtained in the SSE simulations in the standard way using the fluctuation of the winding numbers.^{22,23} Again, the finite-size behavior should be very different for a continuous $z=1$ phase transition and for a first-order transition. In the former case, $\rho_s \sim 1/L$ for large enough system sizes at the critical coupling. Thus, $\rho_s L$ curves for different system sizes intersect at the critical coupling for a $z=1$ continuous critical point, given L is sufficiently large. However, at a first-order transition, since there is phase coexistence, ρ_s is finite (nonzero) at the transition point when $L \rightarrow \infty$ and thus $\rho_s L \rightarrow \infty$ as the system size is increased and no unique crossing point is obtained. Figure 4 shows the behavior of both ρ_s and $\rho_s L$. Intersection between $\rho_s L$ curves for different L can indeed be seen close to the transition point but the value at the intersection points (e.g., L and $L+2$) increases with L . The ρ_s curves become sharper and approach a step function with a discontinuity at $(Q_3/J)_c$ as L increases. Inter-

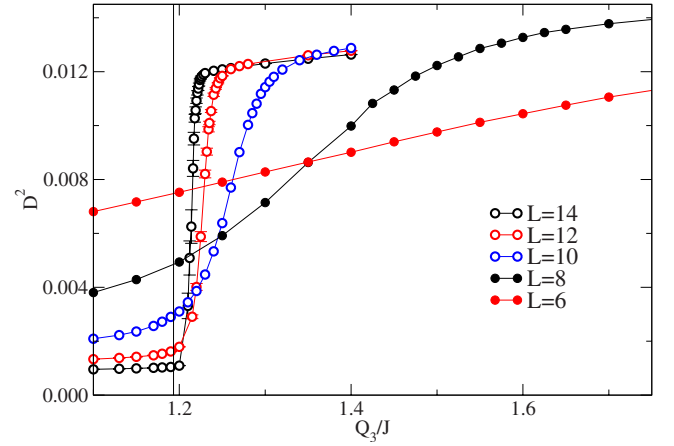


FIG. 5. (Color online) Size dependence of the VBS order parameter D^2 for different system sizes.

estingly, the spin stiffness ρ_s actually increases on approaching the transition from the Néel phase before sharply dropping off in the VBS phase.

B. VBS order

To provide further evidence for the first-order nature of the transition, and to obtain a bench mark for the finite-size scaling, it is useful to also consider observables sensitive to the VBS order. We define the following order parameters for that purpose:

$$D_x = \frac{1}{N} \sum_{\mathbf{r}} S^z(\mathbf{r}) S^z(\mathbf{r} + \hat{\mathbf{x}}) \cos(\mathbf{Q} \cdot \mathbf{r}), \quad (7)$$

$$D_y = \frac{1}{N} \sum_{\mathbf{r}} S^z(\mathbf{r}) S^z(\mathbf{r} + \hat{\mathbf{y}}) \cos(\mathbf{Q} \cdot \mathbf{r}), \quad (8)$$

$$D^2 = \langle D_x^2 + D_y^2 \rangle, \quad (9)$$

where again $\mathbf{Q}=(\pi, \pi)$. The squared order parameter D^2 is zero in the Neel phase and becomes nonzero in the VBS phase in the thermodynamic limit. In Fig. 5, we show the behavior of D^2 near the transition. The jump in D^2 gets sharper with increasing system size, similar to the staggered magnetization in Fig. 2, and its location approaches $(Q_3/J)_c$. Thus, the solid order parameter also shows a first-order transition. Note that the order parameter we use here is not spin-rotationally invariant. One can also define D_x and D_y using rotationally invariant bond operators such as $\mathbf{S}(\mathbf{r}) \cdot \mathbf{S}(\mathbf{r} + \hat{\mathbf{x}})$. There may be differences in the finite-size scaling properties¹³ but for our purposes here the rotational invariance is not necessary (and the z -component definition of D^2 is easier to measure with the SSE method).

A strong signature of a first-order transition is phase coexistence at the transition point, unlike in the case of a continuous transition. We already showed evidence of coexistence of a Néel and nonmagnetic phase in the form of a negative Binder cumulant of the staggered magnetization in Fig. 2. The coexistence can be observed in a more direct way

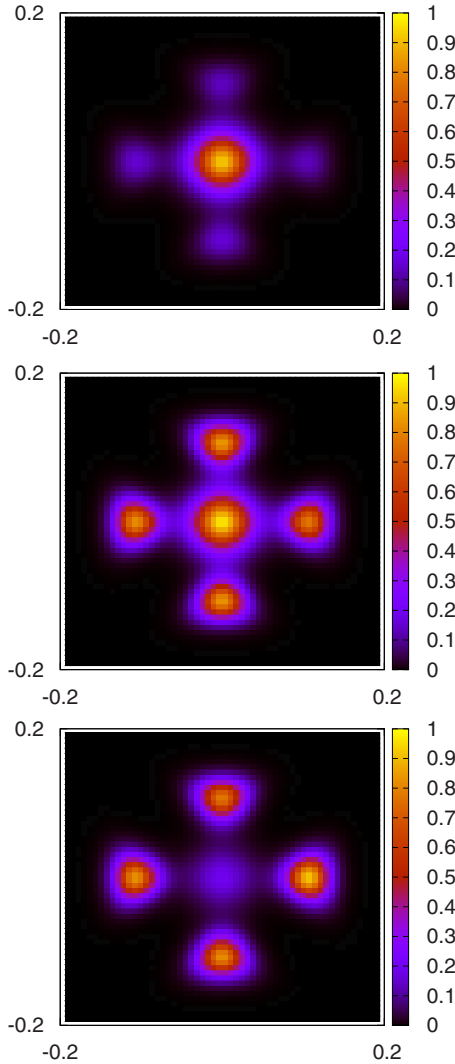


FIG. 6. (Color online) The probability density $P(D_x, D_y)$ shown for $L=12$ at $Q_3/J=1.22, 1.23, 1.24$ (from top to bottom) and $\beta J = 12$. The maxima present both at $(0,0)$ and $(\pm D, 0), (0, \pm D)$ at $Q_3/J=1.23$ show phase coexistence of the Néel and VBS orders.

using the VBS order parameter. Consider the joint probability distribution function $P(D_x, D_y)$. In the Néel phase, this function is peaked at $(0,0)$. In the VBS phase, $P(D_x, D_y)$ is peaked at $(0, \pm D)$ and $(\pm D, 0)$, where D is finite, reflecting the Z_4 degeneracy of the VBS state in a finite lattice. Note that (D_x, D_y) is here defined as a single point obtained on the basis of an equal-time simultaneous measurement of D_x and D_y , i.e., these operators are not averaged over the imaginary-time dimension in the simulations. The full distribution can still of course be accumulated over several imaginary times.

In Fig. 6, we show $P(D_x, D_y)$ for $L=12$ and $Q_3/J = 1.22, 1.23, 1.24$ for $\beta J = L$. The coexistence of the Néel and the VBS phase is evident from the presence of peaks at both $(0,0)$ and $(\pm D, 0), (0, \pm D)$ at $Q_3/J=1.23$ while at $Q_3/J = 1.22$ ($Q_3/J=1.24$), the Néel (VBS) phase dominates. Also note the absence of any $U(1)$ ringlike feature in the distribution shown in Fig. 6. This should be contrasted with similar measures of the distribution function in the J - Q models with columnar VBS states close to the critical point, where the

enlarged $U(1)$ symmetry is very evident.^{9,10,14} In the original J - Q model with two singlet projectors, the VBS does not seem to get pinned to the four Z_4 symmetric angles even at $J=0$ for the system sizes accessible.⁹ In the modified J - Q model with three singlet projectors forming columns,¹⁰ the change in the shape of the VBS order-parameter distribution from $U(1)$ close to the transition to Z_4 deep in the VBS phase can be clearly observed, however. The enlarged $U(1)$ symmetry arises in DQC theory due to the (dangerously) irrelevant Z_4 symmetry-breaking term at the critical point.² Away from the critical point, the symmetry is only approximate but *large* system sizes are needed to observe that (i.e., L has to exceed the length scale Λ which is larger than the standard correlation length and determined by the dangerously irrelevant operator).

Within the DQC framework, the approximate $U(1)$ symmetry near the critical point can be thought of in the following manner:² the dangerously irrelevant Z_4 perturbation only produces a small energy difference between the columnar and plaquette VBS, which vanishes at the critical point and gives rise to a corresponding large length scale slightly away from it within which the magnitude of the VBS order parameter is formed but its angle (which can be defined exactly as we did above in terms of D_x and D_y) is not pinned in any particular direction. This feature has also been observed in $U(1)$ symmetric spin models where either a very *weak* first-order transition²⁴ or transition with *unusual* finite-size scaling²⁵ takes place. However, when the VBS is staggered, there is no competing solid that is energetically close because of the absence of local ring exchange moves of the singlets (or dimers) in the ideal staggered solid. This does not allow the emergence of an approximate $U(1)$ symmetry near the transition, for which local fluctuations of the VBS order parameter are necessary, and puts it outside the framework of DQC points even though the phases have the same broken symmetries. Note that the value of D^2 in the VBS phase after the discontinuous jump (Fig. 5) is *close* ($\sim 74\%$) to that of an ideal staggered solid ($D^2=0.015625$), which motivates us to classify it as a strongly first-order transition.

We should point out here that the order-parameter distribution $P(m_s^z)$ of the Néel order parameter does not show a clear peak structure at coexistence because of the spin-rotational averaging when measuring just one of the three components of the staggered magnetization. The distribution is not sharply peaked in the Néel state. In principle one could measure deviations from the rotationally averaged distribution expected²⁶ for a single phase but this signal is not as clear as the one seen above for the VBS order parameter. In the Binder cumulant this problem is avoided because only even powers of m_s are used and they can be trivially related to the corresponding powers of m_s^z . In principle one could also measure the x and y components of the staggered structure factor, and compute the distribution $P(|m_s|)$, but since these are off-diagonal operators in the basis used there are ambiguities in how to define m_s^x and m_s^y for a given configuration in which m_s^z is also measured.

III. DETERMINATION OF THE TRANSITION POINT

The location of a phase transition in the thermodynamic limit may be determined by using finite-size scaling argu-

ments. For first-order transitions at finite temperature, the peak position of the specific heat C_v , susceptibility χ , and the minimum of the Binder cumulant of the order-parameter approaches²⁷ the thermodynamic transition temperature $T_c(L \rightarrow \infty)$ as L^{-d} , where d is the dimensionality of the system. However, it is known from numerical studies of classical phase transitions (e.g., in $q > 4$ Potts models in 2D) that large system sizes may be needed to observe this *simple* scaling of $T_c(L)$. For example, in Ref. 28, both the $q=8$ and $q=10$ Potts model (both of which exhibit first-order transitions) were studied for $L \leq 50$, and strong deviations from the L^{-d} scaling was observed for the $q=8$ case at these system sizes. Continentino and Ferreira²⁹ have proposed that for a quantum phase transition, similar definitions of $g_c(L)$ will approach $g_c(L \rightarrow \infty)$ as $L^{-(d+z)}$, where g is the (nonthermal) parameter driving the quantum phase transition and z is a dynamic exponent (this reflects the equivalence of the d -dimensional quantum model at $T=0$ to a $(d+z)$ -dimensional classical model at finite temperature). In our problem, the presence of Néel order at the critical point and using the geometry with $\beta J = L$ imply that finite-size scaling is governed by low-energy linearly dispersing spin waves and therefore $z=1$. The location of the minimum of the Binder cumulant U_2 can be taken as a possible definition for such a pseudocritical coupling $g_c(L)$. With this definition, we have not been able to check the above-mentioned scaling for our model explicitly because of limited system sizes, i.e., the data do not follow pure power laws. To obtain reliable data for bigger system sizes near the critical point, where the tunneling time between the competing phases becomes very large, will possibly require extended ensemble methods (which have been developed for quantum system in Refs. 30–32), which we leave for future work.

Interestingly, the long tunneling times associated with strong first-order transitions can actually be used to locate the value of the critical point accurately. This can be done by determining the average energy of the two different phases³³ in the following manner. To determine the energy of the Néel phase, we start the simulation at a value of Q_3/J inside that phase and then keep increasing Q_3/J to go to the VBS phase while measuring the average energy at each such Q_3/J . In this sequence, we always use the last configuration generated in the run at a particular Q_3/J as the starting seed for the next value of Q_3/J . Given the system is sufficiently big so that the tunneling time is large compared to the simulation time, this procedure ensures that the system stays in the *metastable* Néel phase close to the critical point even when it has been crossed. We then repeat this process in the reverse direction starting from a value of Q_3/J inside the VBS phase and decreasing the value of Q_3/J . The crossing point of the two energy branches then gives the location of a pseudocritical coupling $(Q_3/J)_c(L)$ at that system size. In Fig. 7 (top panel), we show the results of this procedure for $L=36$. The curves can be fitted very well to quadratic polynomials (the small quadratic part is added to improve χ^2/DOF) and the crossing point can be accurately determined. These crossing points are indeed consistent with a scaling of the form $(Q_3/J)_c(L) = (Q_3/J)_c - A/L^3$ for the larger system sizes studied ($L=24-36$) [see Fig. 7 (bottom panel)] assuming that $z=1$. We obtain $(Q_3/J)_c = 1.1933(1)$ using this extrapolation.

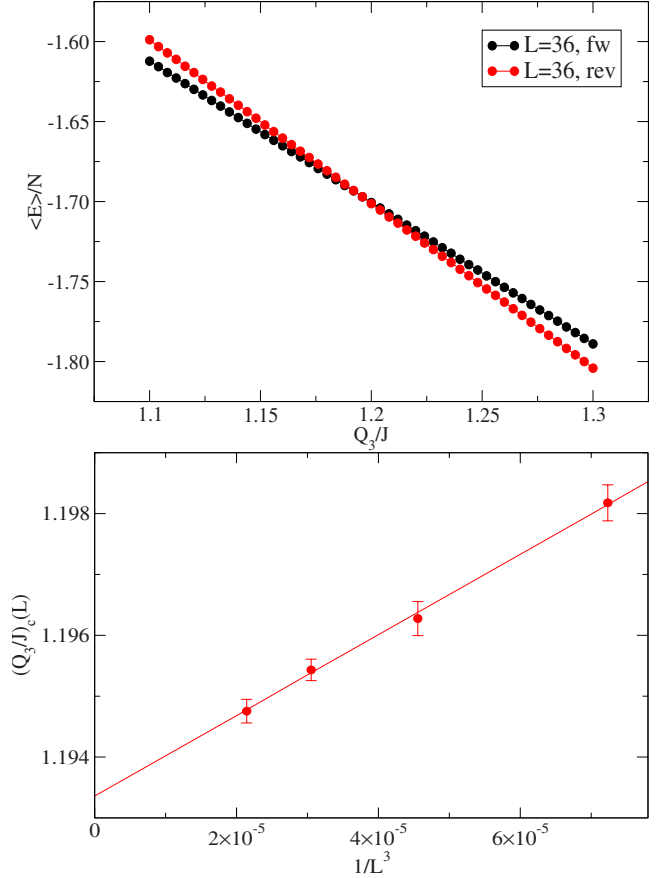


FIG. 7. (Color online) Critical coupling $(Q_3/J)_c(L)$ extracted from the crossing of the energy branches (top panel) of the Néel phase (labeled as fw) and the VBS phase (labeled as rev) for a system of size $L=36$ at $\beta J=36$. The bottom panel shows a fit to the form $(Q_3/J)_c(L) = (Q_3/J)_c + A/L^3$ to extract the thermodynamic value of $(Q_3/J)_c = 1.1933(1)$.

IV. CONCLUSION

In conclusion, we have considered a modified “ J - Q_3 ” type Hamiltonian, where the Q_3 term is chosen to stabilize a staggered VBS solid. We demonstrate the presence of a strong first-order quantum critical point that separates the Néel and the VBS phases. In the VBS phase, there is no approximate $U(1)$ symmetry and associated ringlike features in the probability distribution of the VBS order parameter close to the critical point. We also use the crossing of the energy branches of the two phases for larger system sizes to estimate the thermodynamic value of the critical point. We observe that these crossing points (for $L=24-36$) indeed converge to the thermodynamic value of the critical point as $1/L^3$, expected from finite-size scaling for first-order transitions with $\beta \sim L$. It will be interesting to test similar predictions of finite-size scaling theory of first-order quantum phase transitions,²⁹ which should depend solely on the dimensionality of the system d and the dynamical exponent z , by measuring the order parameters and the Binder cumulant using quantum Monte Carlo simulations in combination with extended ensemble methods^{30–32} for bigger systems that may avoid the large tunneling times between the two coexisting

phases near the transition. It will also be interesting to see whether there is a finite temperature crossover to a continuous phase transition between a VBS and a disordered phase. Given the strong first-order nature of the transition, it will likely survive at low T as well. Though the transition is strongly first order, there are still fluctuations present near the critical point, e.g., D^2 is 74% of its maximal value in the VBS phase in the vicinity of the transition and the length scale of appearance of first-order signatures in the Binder cumulant of the staggered magnetization is $L \approx 4$. Mean-field theories^{34,35} have not been successful for the original J - Q model. It will be interesting to see whether a reasonable description of this transition and its location can be obtained using similar techniques (e.g., mean-field theory based on bond-operator formulation for $S=1/2$ introduced by Sachdev

and Bhatt in Ref. 36) and this is presently being investigated. Finally, none of the finite-size signatures of first-order transitions, such as negative divergence of the Binder cumulant, crossing of energy branches, etc., presented in this study, have been observed in previous simulations of $SU(2)$ symmetric J - Q type models with a columnar VBS phase even for very large system sizes (L up to 256).¹⁵

ACKNOWLEDGMENTS

The authors would like to acknowledge useful discussions with F. Alet, K. Damle, R. K. Kaul, and R. G. Melko. This work is supported by the NSF under Grant No. DMR-0803510.

-
- ¹S. Sachdev, *Quantum Phase Transitions* (Cambridge University Press, Cambridge, England, 1999).
 - ²T. Senthil, A. Vishwanath, L. Balents, S. Sachdev, and M. P. A. Fisher, *Science* **303**, 1490 (2004); T. Senthil, L. Balents, S. Sachdev, A. Vishwanath, and M. P. A. Fisher, *Phys. Rev. B* **70**, 144407 (2004); M. Levin and T. Senthil, *ibid.* **70**, 220403 (2004).
 - ³N. Read and S. Sachdev, *Phys. Rev. Lett.* **62**, 1694 (1989).
 - ⁴G. Murthy and S. Sachdev, *Nucl. Phys. B* **344**, 557 (1990).
 - ⁵A. B. Kuklov, N. V. Prokof'ev, and B. V. Svistunov, *Phys. Rev. Lett.* **93**, 230402 (2004).
 - ⁶A. B. Kuklov, M. Matsumoto, N. V. Prokof'ev, B. V. Svistunov, and M. Troyer, *Phys. Rev. Lett.* **101**, 050405 (2008).
 - ⁷O. Motrunich and A. Vishwanath, *Phys. Rev. B* **70**, 075104 (2004); arXiv:0805.1494 (unpublished).
 - ⁸S. Takashima, I. Ichinose, and T. Matsui, *Phys. Rev. B* **72**, 075112 (2005).
 - ⁹A. W. Sandvik, *Phys. Rev. Lett.* **98**, 227202 (2007).
 - ¹⁰J. Lou, A. W. Sandvik, and N. Kawashima, *Phys. Rev. B* **80**, 180414(R) (2009).
 - ¹¹P. Henelius and A. W. Sandvik, *Phys. Rev. B* **62**, 1102 (2000).
 - ¹²P. Chandra and B. Douçot, *Phys. Rev. B* **38**, 9335 (1988); A. V. Chubukov, *ibid.* **44**, 392 (1991); E. Dagotto and A. Moreo, *Phys. Rev. Lett.* **63**, 2148 (1989); M. P. Gelfand, R. R. P. Singh, and D. A. Huse, *Phys. Rev. B* **40**, 10801 (1989).
 - ¹³R. G. Melko and R. K. Kaul, *Phys. Rev. Lett.* **100**, 017203 (2008).
 - ¹⁴F.-J. Jiang, M. Nyfeler, S. Chandrasekharan, and U.-J. Wiese, *J. Stat. Mech.: Theory Exp.* (2008), P02009.
 - ¹⁵A. W. Sandvik, *Phys. Rev. Lett.* **104**, 177201 (2010).
 - ¹⁶A. Banerjee, K. Damle, and F. Alet, arXiv:1002.1375 (unpublished).
 - ¹⁷D. H. Kim, P. A. Lee, and X.-G. Wen, *Phys. Rev. Lett.* **79**, 2109 (1997).
 - ¹⁸A. W. Sandvik, *Phys. Rev. B* **59**, R14157 (1999); O. F. Syljuåsen and A. W. Sandvik, *Phys. Rev. E* **66**, 046701 (2002).
 - ¹⁹K. Binder, *Phys. Rev. Lett.* **47**, 693 (1981); K. Binder and D. P. Landau, *Phys. Rev. B* **30**, 1477 (1984).
 - ²⁰K. Vollmayr, J. D. Reger, M. Scheucher, and K. Binder, *Z. Phys. B: Condens. Matter* **91**, 113 (1991).
 - ²¹O. Cépas, A. P. Young, and B. S. Shastry, *Phys. Rev. B* **72**, 184408 (2005).
 - ²²E. L. Pollock and D. M. Ceperley, *Phys. Rev. B* **36**, 8343 (1987).
 - ²³A. W. Sandvik, *Phys. Rev. B* **56**, 11678 (1997).
 - ²⁴A. Sen, K. Damle, and T. Senthil, *Phys. Rev. B* **76**, 235107 (2007).
 - ²⁵A. W. Sandvik and R. G. Melko, *Ann. Phys. (N.Y.)* **321**, 1651 (2006).
 - ²⁶U. Gerber, C. P. Hofmann, F.-J. Jiang, M. Nyfeler, and U.-J. Wiese, *J. Stat. Mech.: Theory Exp.* (2009), P03021.
 - ²⁷M. E. Fisher and A. N. Berker, *Phys. Rev. B* **26**, 2507 (1982).
 - ²⁸J. Lee and J. M. Kosterlitz, *Phys. Rev. B* **43**, 3265 (1991).
 - ²⁹M. A. Continentino and A. S. Ferreira, *Physica A* **339**, 461 (2004).
 - ³⁰P. Sengupta, A. W. Sandvik, and D. K. Campbell, *Phys. Rev. B* **65**, 155113 (2002).
 - ³¹M. Troyer, S. Wessel, and F. Alet, *Phys. Rev. Lett.* **90**, 120201 (2003).
 - ³²S. Trebst, D. A. Huse, and M. Troyer, *Phys. Rev. E* **70**, 046701 (2004).
 - ³³R. G. Melko, A. W. Sandvik, and D. J. Scalapino, *Phys. Rev. B* **69**, 100408(R) (2004).
 - ³⁴L. Isaev, G. Ortiz, and J. Dukelsky, *J. Phys.: Condens. Matter* **22**, 016006 (2010).
 - ³⁵V. N. Kotov, D.-X. Yao, A. H. Castro Neto, and D. K. Campbell, *Phys. Rev. B* **80**, 174403 (2009).
 - ³⁶S. Sachdev and R. N. Bhatt, *Phys. Rev. B* **41**, 9323 (1990).